Available online at www.sciencedirect.com
ScienceDirect
Journal of Molecular Catalysis A: Chemical 281 (2008) 107–112
JOURNAL OF MOLECULAR CATALYSIS A: CHEMICAL
www.elsevier.com/locate/molcata

Photocatalytic degradation of 2,4-dichlorophenoxyacetic acid using nanocrystalline cryptomelane composite catalysts

M. Alvarez Lemus [a,b], T. López [a,b], S. Recillas [a,b,*], D.M. Frías [c], M. Montes [c], J.J. Delgado [d], M.A. Centeno [e], J.A. Odriozola [e]

[a] *Departamento de Química, Universidad Autónoma Metropolitana-Xochimilco, 1100 Calzada del Hueso, México D.F. 04960, Mexico*
[b] *Nanotechnology Laboratory, National Institute of Neurology and Neurosurgery, Insurgentes Sur 3877, Mexico D.F. 14269, Mexico*
[c] *Applied Chemistry Department, University of the Basque Country (UPV-EHU), P. Lardizabal 3, San Sebastián 20018, Spain*
[d] *Dep. de Ciencia de los Materiales e Ingeniería Metalúrgica y Química, Inorgánica de la Universidad de Cádiz, C/. República Saharaui s/n, Aptdo. 40, Puerto Real, Cádiz, Spain*
[e] *Department of Inorganic Chemistry and Materials Science Institute, Universidad de Sevilla – CSIC, Av. Américo Vespucio No. 49, Sevilla 41092, Spain*

Available online 17 November 2007

Abstract

2,4-Dichlorophenoxyacetic acid is a common systemic herbicide used in the control of broadleaf weeds. It is the third-most widely used herbicide in the world. 2,4-D heterogeneous photocatalysis has emerged as a useful process to aid remediation of wastewater contamination. Manganese oxide with 2×2 tunnel structure, cryptomelane show good results in the photodegradation of 2,4-D and excellent performance in the photodegradation of methylene blue. The later as a consequence of the S–Mn interaction that favours the adsorption step in the photodegradation process. The existence of microporous manganese oxide minerals with the OMS structure may be an acceptable environmental solution for the remediation of wastewaters.

Keywords: Photocatalytic degradation; Cryptomelane; 2,4-Dichlorophenoxyacetic acid; Methylene blue

1. Introduction

Actually, one of the major concerns of human beings is the contamination of water resources. The extensive use of pesticides in agriculture is compromising soil and water quality. 2,4-dichlorophenoxyacetic acid (2,4-D) is the most widely used herbicide in the world and is the third-one employed in North America. There are over 1500 pesticide and herbicide products that contain 2,4-D as the main ingredient. The U.S. EPA Office of Pesticide Programs estimated that total domestic U.S. annual usage of 2,4-D is approximately 46 million pounds with 66% of use in agricultural applications. Exposure to 2,4-D has been reported to result in blood, liver, and kidney toxicity. Chronic oral exposure in experimental animals has resulted in adverse effects on the eye, thyroid, kidney, adrenals, and ovaries/testes [1]. An important alternative to degradation of the 2,4-D is the photocatalytic processes. In this work, MnO_x type cryptomelane (coexistence of Mn^{III} and Mn^{IV}) was used as photocatalyst (Fig. 1). This oxide was used in many chemical processes due to their porous structure, mild surface acidity–basicity and ion-exchange ability [2–5]. Cryptomelane, one of the members of the manganese oxide OMS-2 group (octahedral molecular sieve) present a 2×2 tunnel structure formed by edge-sharing [MnO_6] octahedra that forms channels of different size depending on the combination of the octahedral structures [6]. These compounds are ionic solids showing electrical conductivity and they have the possibility of accommodating cations inside the tunnels. Cryptomelane has been reported to have excellent catalytic properties [10], and has been extensively tested in NOx-SCR with ammonia [12], phenol wet oxidation [4] and VOC's abatement [5,8]. Microporous manganese oxide minerals act as important chemical controls in soils and sediments and associated water systems, and with their synthetic analogs they are valued for their catalytic, ion exchange, electrochemical, and adsorption properties. A natural deposit of this cryptomelane mineral is known as the La Hueca mine situated in northwestern Michoacán,

* Corresponding author. Tel.: +52 222 2477344.
E-mail address: recillas06@yahoo.com.mx (S. Recillas).

1381-1169/$ – see front matter © 2007 Elsevier B.V. All rights reserved.
doi:10.1016/j.molcata.2007.10.037

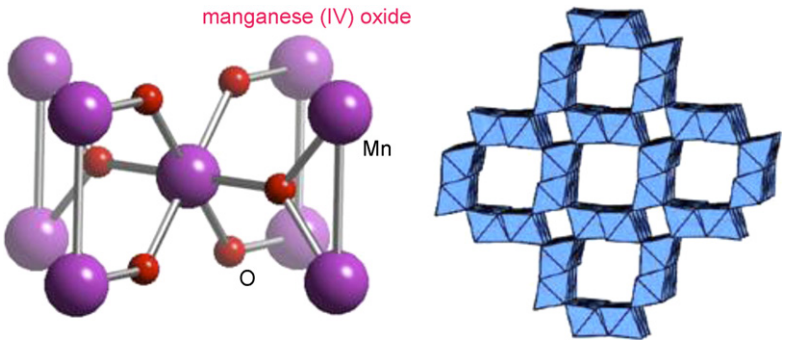

Fig. 1. Coordination sphere of manganese and octahedron arrangement in crytomelane type oxide.

4 km east of La Minita volcanogenic sulphide deposit. Other members of this family as woodruffite, a 3×4 tunnel zinc manganese oxide hydrate, are also present as mineral deposits in México.

In this work, we studied photocatalytic properties of manganese oxide (cryptomelane) in the photodegradation of 2,4-D and methylene blue using ultraviolet radiation. Methylene blue is a heterocyclic aromatic chemical compound with molecular formula: $C_{16}H_{18}ClN_3S$. It has many uses in a range of different fields, such as biology and chemistry. At room temperature, it appears as a solid, odorless, dark green powder that yields a blue solution when dissolved in water.

2. Experimental

2.1. Synthesis

The reflux method used to prepare cryptomelane was first proposed by Luo et al. [10]. Briefly, 11 g of $MnAc_2{\cdot}4H_2O$ (Aldrich) were dissolved in 40 ml of a buffer solution containing 5 ml of glacial acetic acid and 5 g of KAc in 40 ml of double distilled water (DDW). To this buffered solution 150 ml of DDW containing 6.5 g of $KMnO_4$ (Aldrich) was added slowly while stirring and further refluxed under continuous stirring for 24 h (pH 4.5). At the end of the synthesis procedure the obtained solid was filtered, washed, dried at 120 °C for 30 min, and finally calcined in air at 450 °C for 2 h.

2.2. Characterization

The X-ray powder diffraction patterns of the samples were collected using a Phillips PW 1729–1820 instrument using Cu Kα radiation (45 kV and 40 mA). The crystal phases were identified using the PDF2 Database from the International Centre for Diffraction Data. The Scherrer equation was used to estimate the mean crystallite size. The width of the cryptomelane (2 1 1) peaks at half-maximum was corrected for Kα doublet and instrumental broadening [9]. High-resolution transmission electron microscopy (HRTEM) characterization was performed on a 200 kV, JEOL JEM-2011LaB6. The sample was ultrasonically suspended in hexane and deposited on a Cu grid covered with a thin layer of carbon (holey carbon). Nitrogen adsorption measurements were carried out in a Micromeritics ASAP 2020 to determine the textural properties. Specific surface area was calculated according to the BET method, external and microporous area using t-plot, total pore volume from the adsorption at $p/p_0 = 0.98$ and pore size distribution and mean pore size by the BDJH method applied to the desorption branch of the isotherm. Average oxidation state (AOS) of manganese was determined by the redox method, based in double titration with $KMnO_4$. In the first one, the solid was dissolved in HCl and the total amount of manganese measured. In the second one, after reductive dissolution with $(NH_4)_2Fe(SO_4)$ in acid medium (H_2SO_4), the redox equivalents needed to reduce the different manganese species to Mn^{2+} were quantified [11]. The UV–vis spectrum was taken with a Cary-100 Varian spectrophotometer with integration sphere. The pulverized sample was directly observed. The cryptomelane photocatalytic activity was evaluated for the 2,4-D pesticide and methylene blue molecules. The catalytic photodegradation test was performed using the following procedure: 100 mg of cryptomelane were placed in 100 ml of a 50 ppm solution of 2,4-D. For ensuring the adsorption of the molecule on the photocatalyst, the suspension was maintained in the absence of light under continuous stirring for 1 h while flowing air (1 ml/s). Immediately, the suspension was submitted to a sealed container for subsequent irradiation using a low pressure Hg lamp (UVP 90001201, with typical intensity of 4400 μW/cm^2, emitting a radiation of 254 nm). In order to follow the photodegradation, samples were collected at regular intervals and analysed using UV–vis spectroscopy. Each sample was filtered through a nylon membrane (0.45 μm) to remove the oxide particles before analysis. UV probes without catalyst were performed in both cases. Methylene blue (MB), 20 ppm, photodegradation was studied using cryptomelane and TiO_2 (P-25 Degussa) calcined at 500 °C.

3. Results and discussion

The X-ray diffraction pattern of cryptomelane material is shown in Fig. 2. All possible reflections of cryptomelane (JCPDS 29-1020) are present with characteristic reflections (angle position $2\theta = 12.8°$, 18.5°, 28.9°, 37.5°, 42°, and 50°) [7] and the peak broadness is indicative of the small crystal size. Fig. 2 shows that cryptomelane diffraction peaks are sharper in the material prepared by Luo et al. [10]. Electron microscopy images (Fig. 3) show fibers presenting diameters between 10 and 20 nm

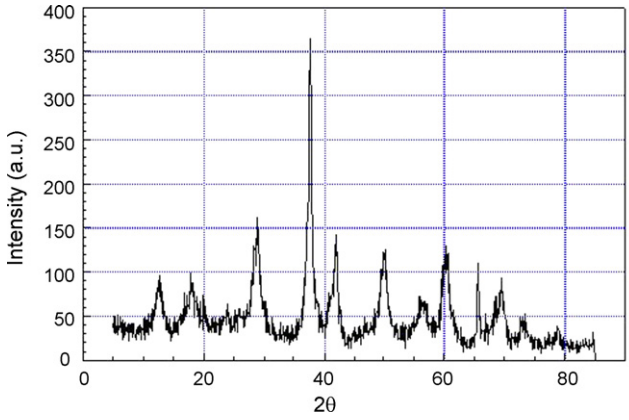

Fig. 2. X-ray diffraction pattern of the prepared oxide.

(19.6 nm in Fig. 3b) with a high aspect ratio ($L/D \approx 10$–20). The diameter observed agrees with the average crystallite size calculated by XRDLB, 15.4 nm. The formation of these fibers has been reported to depend on the aging time and temperature [10], and the ones obtained in our case are as small in size as the ones reported in the literature for another synthesis of cryptomelane. The fiber morphology is represented in Fig. 3a and details in Fig. 3b–d. The sample presents nanofiber bunch morphology. High-resolution transmission electron microscopy (HRTEM) images suggest the (1 1 0) orientation of the fibers. At the end of one fiber, it can see the 2×2 tunnel structure of nanosized cryptomelane (Fig. 3d).

Nitrogen adsorption–desorption isotherms and pore size distributions (PSD) are shown in Fig. 4. The isotherms recorded for these nanomaterials correspond to Type IV adsorption isotherms with a steep increase at low p/p_0 and capillary condensation at high p/p_0 and (p and p_0 are the adsorption and saturation vapor pressure of N_2 at 77 K, respectively). Micropore filling of Type I adsorption isotherm occurs at low p/p_0, suggesting the existence of micropore in the nanomaterials in addition to the mesoporosity confirmed by the hysteresis loop at high p/p_0. The hysteresis loop is Type H1 for all nanomaterials, according to IUPAC classifications suggesting the existence of cylindrical or constant cross-section pores. The pore size distribution of the K-OMS material shows a Gaussian curve form centered at 30 nm. Table 1 summarize the main textural parameters obtained from these nitrogen isotherms: BET surface area (S_{BET} in m^2/g), external surface area (S_{ext} in m^2/g), micropore sur-

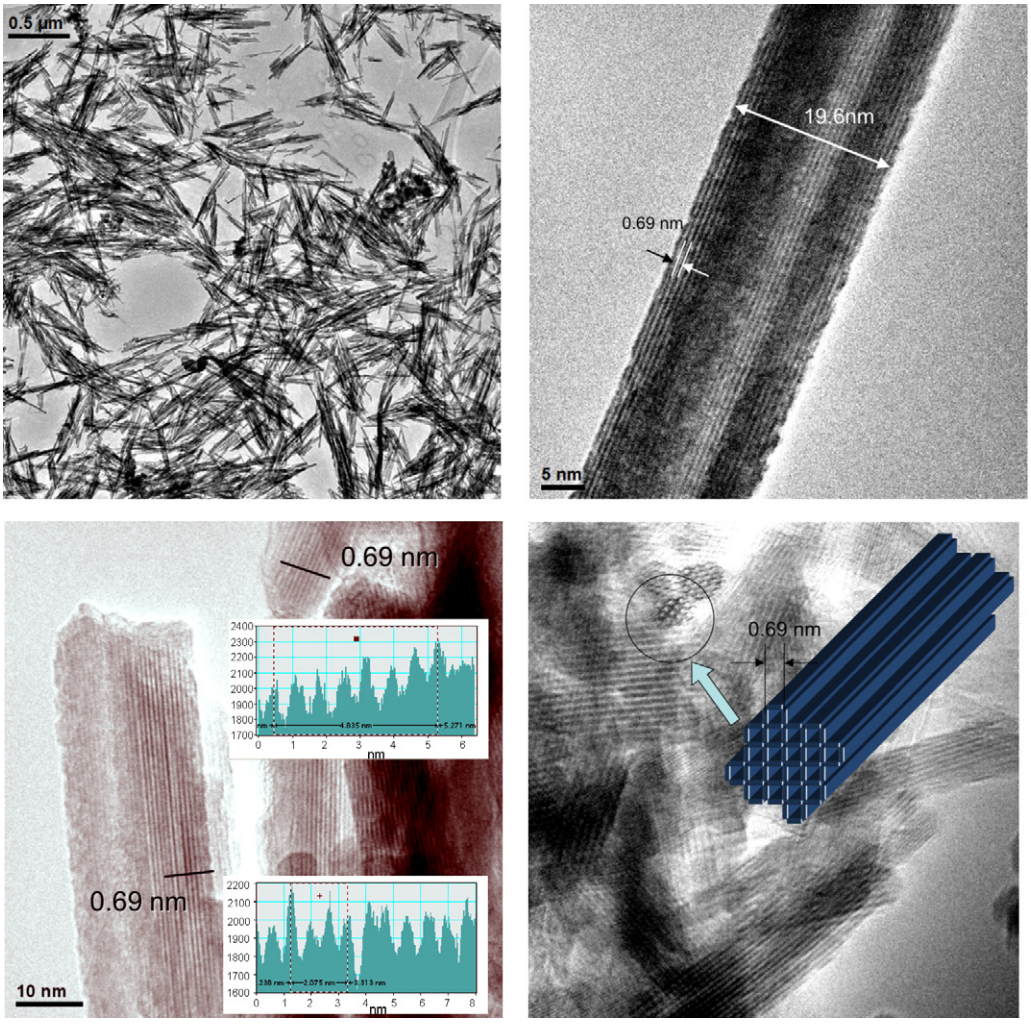

Fig. 3. TEM images at low (a) and high magnification (b–d).

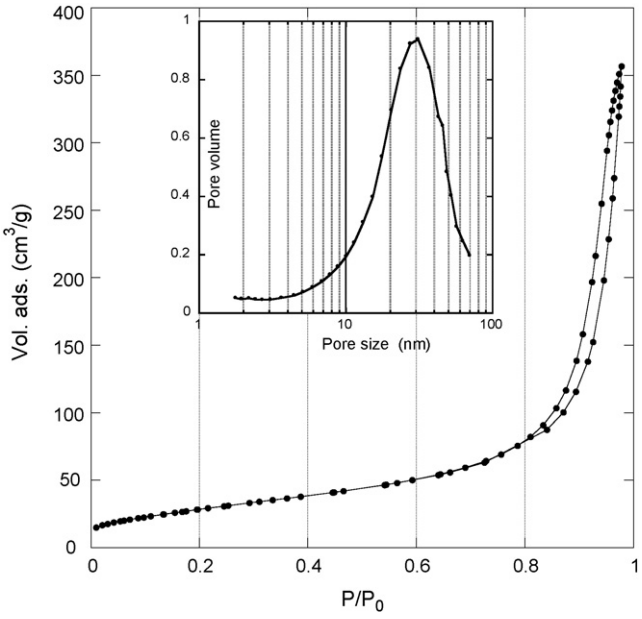

Fig. 4. N_2 adsorption isotherm plot of crytomelane. The inset shows the pore size distribution plot obtained through the BDJH method.

face area (S_μ in m^2/g), and micropore volume ($V_{\mu p}$ in cm^3/g) obtained from t-plots, total pore volume (V_p in cm^3/g), and mean pore diameter (nm) obtained from the pore size distribution [8]. Micropore surface area is only 10% of the total surface area, and micropore volume represents less than 2% of the total pore volume. Therefore, the excellent textural properties of this material are due to the accessibility of the external surface of the nanofiber and the pore volume comes from the space between fibers. The space inside the cryptomelane tunnels is no available for nitrogen molecules, and less to other larger reactant molecules.

The average oxidations state of manganese measured in our criptomelane by redox titration is 3.8. Accepting that Mn^{3+} and Mn^{4+} are the only oxidation states [20] it can be estimated 20% Mn^{3+} and 80% Mn^{4+}. UV–vis spectrum (Fig. 5) also provides information on the oxidation state of manganese. The spectrum of cryptomelane consists of six bands. In the UV region two charge transfer (CT) bands at 250 and 303 nm region can be observed, the later due to electron transfer between manganese d orbitals and oxygen s orbitals, ascribed to $O^{2-} \rightarrow Mn^{3+}$ charge-transfer transitions. The 250 nm band is characteristic of

Table 1
Textural properties of cryptomelane and average oxidation state of manganese

Surface area	
S_{BET} (m^2/g)	125
S_{ext} (m^2/g)	113
S_μ (m^2/g)	12
Pore volume	
V_p (cm^3/g)	0.33
$V_{\mu p}$ (cm^3/g)	0.004
Pore size (nm)	30
AOS	3.8

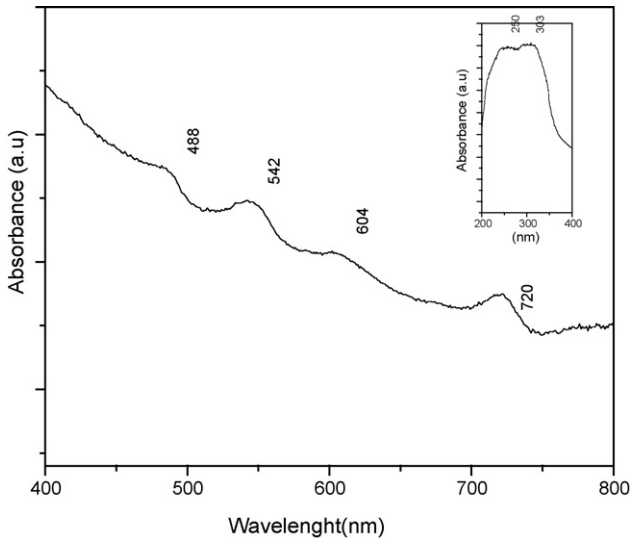

Fig. 5. UV–vis adsorption spectrum of cryptomelane.

the $O^{2-} \rightarrow Mn^{2+}$ charge-transfer. The Mn^{2+} and Mn^{3+} species coexist in this sample. Two bands appear at 488 and 542 nm assigned to the one electron orbital transition $^2t_{2g}$ (↑) → ^3e_g (↑) in Mn^{+4} and $^5E \rightarrow {}^5T_2$ transition in Mn^{3+} species. The band located at 720 nm corresponds to a forbidden transition from $^6A_{1g}(S) \rightarrow {}^4T_{1g}(G)^*$ [13]. This data let us state the coexistence of the three-oxidation states of manganese in our sample modifying slightly the relative proportion between Mn^{3+} and Mn^{4+}.

The photodegradation of 2,4-D was followed over a period of 160 min.

The result of this study is shown in Fig. 6. It was observed that degradation occurs only following the adsorption of UV radiation. Over a 2-h period ca. 50% of the compound could be removed. To make comparisons with other catalysts is always difficult since the surface area and porosity might be different and also the concentration of the contaminant and the catalyst

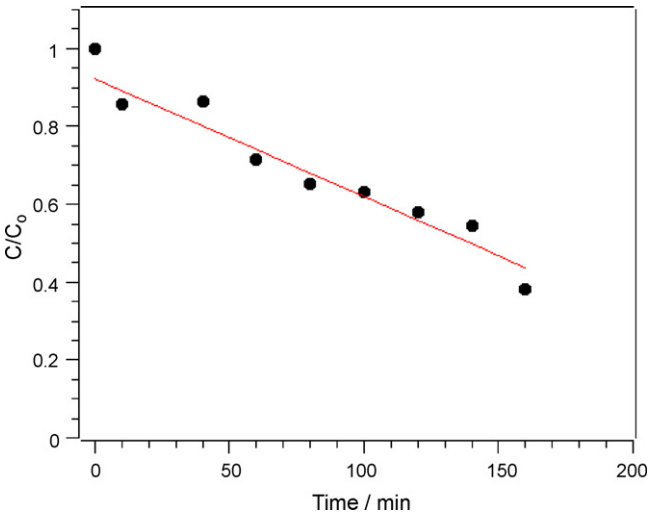

Fig. 6. Catalytic activity of cryptomelane in the photodegradation of 2,4-D.

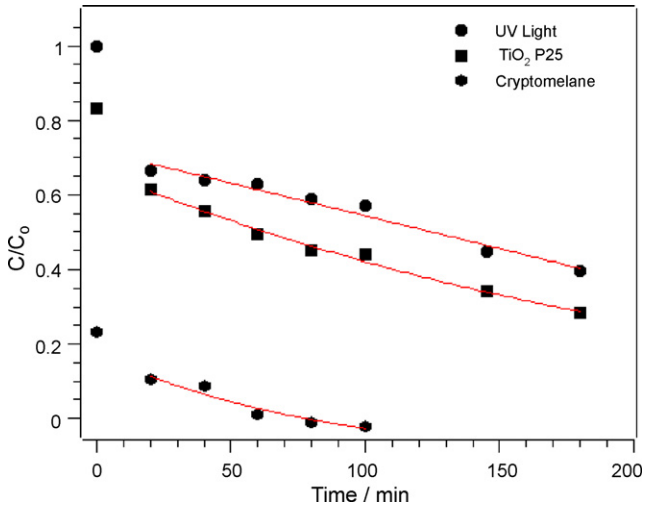

Fig. 7. Catalytic activity of cryptomelane and TiO_2 in the photodegradation of methylene blue.

loading plays a determinant role in the catalyst activity. However, for the sake of comparison it may be considered that for $MnZrO_2$ catalysts 70% of the 2,4-D could be removed in half the time. The behavior of our crytomelane catalyst is similar to that encountered previously for ZrO_2, $FeZrO_2$ and $CoZrO_2$ catalysts whose activity was very similar [14].

The concentration used in this work 2.25×10^{-4} M is one order of magnitude below that used by Piera et al. [15] but we use half of the mass of catalyst with a lower surface area. In these conditions is difficult to compare the catalytic results on the basis of the activity.

If we consider the absolute value and the absence of other oxidants different of the catalyst itself the catalytic performance of our catalyst is worth of being considered. After 60-min reaction cryptomelane catalyst degrades 32.3% of the initial concentration of 2,4-D. Once the solid is continuously irradiated for 160 min 66% of the initial contaminant is degraded. The low performance could be attributed to poor adsorption of the pollutant on cryptomelane. In spite of all of these considerations our catalyst performs better than some iron or anatase catalysts previously reported [16–19].

In order to check this the decomposition of other contaminant has been analysed, in this case the used model 3,7-bis(Dimethylamino)-phenazathionium-chlorideTetramethylthionine chloride ($C_{16}H_{18}ClN_3S$) should strongly adsorb on the cryptomelane surface since the strong affinity of manganese for sulphur.

For this molecule the photodegradation was complete after 70 min in the case of cryptomelane and surprisingly much faster than for the titania catalyst (TiO_2, P-25 Degussa) even thinking that titania has a surface area twice that of the cryptomelane sample (Fig. 7). This effect is related to the strong adsorption of the methylene blue on the cryptomelane surface. In Fig. 7 it is shown that during adsorption in the dark the initial concentration of methylene blue decreases from 20 ppm to a value closer than 5 ppm, that is 75% of the initial concentration is either degraded or adsorbed on the cryptomelane surface. Adsorption experiments in the dark using TiO_2 P25 do not show any significant adsorption after 2 h.

4. Conclusions

Manganese oxides with tunnel structures show catalytic activity in the photodegradation of contaminants. In particular the strong adsorption of methylene blue on manganese oxides due to the strong affinity of manganese for sulphur deserve future interest for this solid. The electronic properties of manganese and the presence of different oxidation states allow use these materials in wastewater treatment. The synthesized cryptomelane presents a better photocatalytic behavior than P-25 and UV light in the degradation of methylene blue. The differences in photocatalytic behavior between 2,4-D and $C_{16}H_{18}ClN_3S$ can be due the polarity of the 2,4-dichlorophenoxyacetic acid, the hydrophobicity of cryptomelane and differences in adsorption capacity between the different contaminants. The performances of the material and the possibility of use natural mineral deposits make this manganese oxide OMS-2 materials well suited for photodegradation of wastewaters.

Acknowledgements

Financial support by UPV/EHU (9/UPV0021.215-14499/2002), MEC (ref. MAT2003-06540), Junta de Andalucía (TEP106, PAI), CONACyT-México, UJAT-PROMEP-México (D.M. Frías PhD Scholarship) is gratefully acknowledged.

References

[1] U.S. Environmental Protection Agency, 2005. "Registration Eligibility Decision for 2,4-D." http://www.epa.gov/oppsrrd1/REDs/.
[2] N. Serpone, E. Pelizzetti (Eds.), Photocatalysis. Fundamental and Applications, Wiley, New York, 1989.
[3] S.L. Suib, Curr. Opin. Solid State Mater. Sci. 3 (1998) 63.
[4] M. Abecassis-Wolfovich, R. Jothiramalingam, M.V. Landau, M. Herskowitz, B. Viswanathan, T.K. Varadarajan, Appl. Catal. B: Environ. 59 (2005) 91–98.
[5] S.L. Brock, N. Duan, Z.R. Tian, O. Giraldo, H. Zhou, S.L. Suib, Chem. Mater. 10 (1998) 2610–2618.
[6] L. Anhuai, G. Xiang, Q. Shan, W. Changqiu, Chin. Sci. Bull. 48 (9) (2003) 920–923.
[7] M.A. Cheney, N.R. Birkner, L. Ma, T. Hartmann, P.K. Bhowmik, V.F. Hodgeb, S.M. Steinberg, Colloid. Surf. A: Physicochem. Eng. Aspect. 289 (2007) 185–192.
[8] D. Frías, S. Nousir, I. Barrio, M. Montes, T. López, M.A. Centeno, J.A. Odriozola, Mater. Charact. 58 (2007) 776–781.
[9] H.P. Klug, L.E. Alexander, X-Ray Diffraction Procedures for Polycrystalline and Amorphous Materials, 2nd ed., John Wiley, New York and London, 1974.
[10] J. Luo, Q. Zhang, A. Huang, S.L. Suib, Micropor. Mesopor. Mater. 35 (2000) 209.
[11] G.-G. Xia, W. Tong, N. Tolentino, N.-G. Duan, S.L. Brock, J.-Y Wang, S.L. Suib, T. Ressler, Chem. Mater. 13 (5) (2001) 1585–1592.
[12] R. Jothiramalingama, B. Viswanathan, T.K. Varadarajana, Mater. Chem. Phys. 100 (2006) 257–261.
[13] P.G. Manning, Can. Miner. 9 (1968) 348–356.
[14] M. Alvarez, T. Lopez, J.A. Odriozola, M.A. Centeno, M.I. Dominguez, M. Montes, P. Quintana, D.H. Aguilar, R.D. Gonzalez, Appl. Catal. B 73 (2007) 34;
C.Y. Kwan, W. Chu, Water Res. 37 (2003) 4405–4412.

[15] E. Piera, J.C. Calpe, E. Brillas, X. Domenech, J. Peral, Appl. Catal. B 27 (2000) 169.
[16] D. Modestov, O. Lev, J. Photochem. Photobiol. A: Chem. 112 (1998) 261–270.
[17] O.M. Alfano, R.J. Brandi, A.E. Cassano, Chem. Eng. J. 82 (2001) 209–218.
[18] Y. Sun, J.J. Pignatello, Environ. Sci. Technol. 27 (1993) 304–310.
[19] M.J. Height, S.E. Pratsinis, O. Mekasuwandumrong, P. Praserthdam, Appl. Catal. B: Environ. 63 (2006) 305–312;
X. Lin, F. Huang, W. Wang, J. Shi, Script. Mater. 56 (2007) 189–192.
[20] J.E. Post, R.B. van Dreele, P.R. Buseck, Acta Crystallogr. B38 (1982) 1056.